High-efficiency metal–semiconductor–metal photodetectors on heteroepitaxially grown Ge on Si

Ali K. Okyay, Ammar M. Nayfeh, and Krishna C. Saraswat

Center for Integrated Systems, Stanford University, Stanford, California 94305

Takao Yonehara

Canon Inc., 30-2, Shimomaruko 3-chome, Ohta-ku, Tokyo 146-8501, Japan

Ann Marshall and Paul C. McIntyre

Department of Materials Science and Engineering, Stanford University, Stanford, California 94305

We demonstrate extremely efficient germanium-on-silicon metal–semiconductor–metal photodetectors with responsivities ($\mathfrak{R}$) as high as 0.85 A/W at 1.55 μm and 2 V reverse bias. Ge was directly grown on Si by using a novel heteroepitaxial growth technique, which uses multisteps of growth and hydrogen annealing to reduce surface roughness and threading dislocations that form due to the 4.2% lattice mismatch. Photodiodes on such layers exhibit reverse dark currents of 100 mA/cm^2 and external quantum efficiency up to 68%. This technology is promising to realize monolithically integrated optoelectronics. © 2006 Optical Society of America

OCIS codes: 230.5160, 130.0250, 130.3130.

Because of its inherent large bandgap, Si is not an efficient optical material at wavelengths in the 1.3–1.55 μm range. Germanium (Ge), with a lower bandgap, is a viable candidate for integration with Si for low-cost transceivers, attracting increasing interest due to its compatibility with Si complementary metal-oxide semiconductors. To integrate Ge onto Si, it is pivotal to develop new methods for heteroepitaxial-Ge technology because Ge growth on Si is hampered by the large lattice mismatch (4.2%). The large mismatch results in growth that is dominated by islanding and misfit dislocations that are formed at the Si substrate/Ge film interface terminating at the film surface as threading dislocations.

Several technologies have been employed to grow Ge heteroepitaxially[1–4] on Si and allow the fabrication of efficient photodetectors. For instance, superlattice buffer layers were used to avoid the large lattice mismatch, and p-i-n Ge detectors on Si with a quantum efficiency of 40% at 1.3 μm were demonstrated.[1] Heteroepitaxial growth followed by cyclic thermal annealing is also a technique to achieve high-quality Ge layers on Si. With such technologies, p-i-n detectors have been built on 4 μm Ge layers grown on Si by using a low-temperature buffer layer,[2] yielding responsivities ($\mathfrak{R}$) ~0.89 A/W at 1.3 μm. Moreover, with this technology, 52% quantum efficiency at 1.3 μm was demonstrated on 1 μm Ge films grown on Si.[3] Using dual strain-relaxed buffer layers, very high 3 dB bandwidth up to 38.9 GHz was demonstrated on vertical p-i-n detectors with 300 nm intrinsic regions.[4]

In this Letter we report the fabrication and demonstration of high-quality Ge-based metal–semiconductor–metal photodetectors (MSM-PDs) by using a recently developed procedure, multiple hydrogen annealing for heteroepitaxy (MHAH),[5] which employs multiple cycles of growth and hydrogen annealing, for growing high-quality heteroepitaxial-Ge layers on silicon. We demonstrate responsivities as high as 0.85 A/W at 1.55 μm and 2 V reverse bias. This technology is promising to realize monolithically integrated optical links as an alternative to electrical interconnects.

We begin the process with standard bulk silicon wafers with resistivity 1–5 $\Omega \times$ cm. The wafers were dipped in 50:1 H_2O:HF (hydrofluoric acid) for 30 s and immediately loaded in an Advanced Semiconductor Materials epitaxial reactor. A hydrogen bake at 950°C was carried out to ensure no native oxide remained on the surface. In the first step, a Ge layer was grown at 400°C at a reduced pressure of 10 Torr. This is followed by hydrogen annealing for 1 h at 825°C and at a pressure of 80 Torr, which yielded ~155 nm of Ge with rms surface roughness of 2.9 nm.[5,6] After the first growth and anneal, a two-step growth process was carried out with only one additional hydrogen anneal with the goal of achieving a thick layer of Ge. The growth temperature was increased to 430°C for 15 min for the first growth step. To further increase the growth rate, the temperature was raised to 500°C for a 15 min duration. Finally, 1 h hydrogen annealing at 700°C completed the process, yielding a 4.5 μm epitaxial Ge layer.

To understand the growth process, in Fig. 1(a) we present a cross-sectional transmission electron micrograph (TEM) image of a two-step MHAH growth that yielded an ~400 nm Ge layer. The image shows that near the surface the dislocation density is reduced, while near the Si/Ge interface the dislocation density is very large. The defect density on top of the layer (100 nm) was extracted to be 2×10^8 cm^{-2} by plan-view TEM [Fig. 1(b)]. The reduction of dislocation density is the result of misfit stress-induced threading dislocation glide, followed by the apparent annihilation of threading segments in the stress-
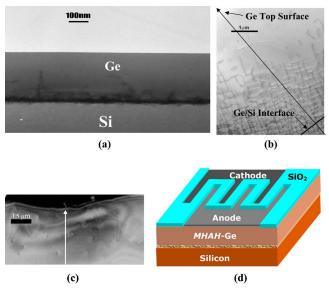
Fig. 1.   (Color online) (a) Cross-sectional TEM image of an ~400 nm heteroepitaxial-Ge layer on Si grown by the MHAH method. (b) Plan-view TEM image of the same layer. As the TEM sample becomes thinner (indicated by arrow), the lower part of the film is increasingly milled away, and only the upper layer of the film, showing drastically reduced defect density, remains. We estimate threading dislocation density of $2 \times 10^8 \, cm^{-2}$ for the upper 100 nm. Dislocations have glided to the Si/Ge interface (arrow indicates the direction away from the Ge/Si interface). (c) Plan-view TEM image of 4.5 μm layer [200 nm from the surface (arrow)]. Dislocation density further was reduced to around $(5-7) \times 10^7 \, cm^{-2}$. (d) Cross-section of MSM photodetector fabricated on MHAH-Ge layer grown on Si starting substrate. SiO$_2$ layer was deposited and patterned before the e-beam evaporation of the metal electrodes. Defects are concentrated near the Si/Ge interface.

relaxed films.[7] Growth of the 4.5 μm layer followed by the final hydrogen anneal reduced the dislocation density to around $(5-7) \times 10^7 \, cm^{-2}$ as confirmed by plan-view TEM [Fig. 1(c)]. In addition, the hydrogen ambient avoids the formation of a surface oxide, allowing for thermally driven Ge surface diffusion to reduce the large surface roughness of the initial layer.[5,6] 1 μm $\times$ 1 μm and 10 μm $\times$ 10 μm atomic-force microscopy scans of the surface yielded a final surface roughness of 0.218 and 2.9 nm, respectively. An x-ray-diffraction (XRD) technique was used to measure residual stress in the films. Contrary to expectations from lattice constant arguments, Ge layers were found to have tensile strain. The tensile strain in the Ge layer can be explained by thermal expansion mismatch with Si substrate and was determined to be~0.17% by XRD measurement.

We used an ~4.5 μm high-quality intrinsic MHAH-Ge layer on Si as the starting substrate. We then fabricated MSM-PDs with interdigitated electrode width and spacing ranging from 1 to 10 μm in active absorption regions of $10^2 - 10^4 \, \mu m^2$. Intrinsic Ge was chosen to allow low-voltage device operation. A 300 nm thick low-temperature chemical-vapor-deposited oxide (LTO) layer was deposited at 400 °C for surface passivation. This oxide layer was patterned and HF-etched followed by metal electrode

e-beam evaporation and photoresist liftoff. Figure 1(d) shows a schematic of the final structure. About 15 nm of Ti, Cr, or Ni were used for work function control and adhesion and topped with ~350 A of Au. No thermal treatments were performed afterward to avoid interdiffusion and alloying between semiconductor and metal.

Metal-semiconductor structures were fabricated and Schottky diode behavior was verified by current–voltage (I–V) characteristics as shown by the inset in Fig. 2, confirming the low defect density of the MHAH-Ge substrates. Figure 2 presents the dark current versus the reverse bias voltage from symmetric MSM-PDs, which show back-to-back Schottky diode behavior. It shows that Cr–Ge–Cr and Ti–Ge–Ti detectors yield similar I_{dark}. We believe the similarity is due to the fact that the work function of Ti and Cr is close to the midgap level of Ge, which produces a high injection barrier for electrons and holes. On the other hand, Ni–Ge–Ni leakage is relatively higher mainly due to a low injection barrier for holes. It should be noted that the MSM-PD structure employed here has not been optimized for I_{dark} suppression. For instance, the large probing pads were in intimate contact with the Ge film together with the interdigitated fingers.

Figure 3 plots $\mathfrak{R}$ versus reverse bias for Ti–Ge–Ti photodetectors operated at 1.55 μm with 330 μm incident intensity. The active absorption area of the device is $10^4 \, \mu m^2$ with 5 μm electrode spacing. We observe $\mathfrak{R}$ of 0.76 A/W under 1 V reverse bias, corresponding to 61% external quantum efficiency (η). The highest $\mathfrak{R}$ of 0.85 A/W, corresponding to η ~68%, was observed from a detector with 5 μm electrode width and spacing. Under similar conditions, the theoretical maximum collection efficiency, for a film of 4.5 μm thick, is 88% without accounting for
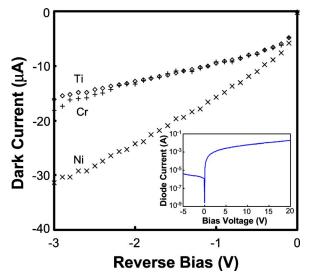

Fig. 2.   (Color online) Measured I_{dark} for symmetric metal–Ge–metal photodiodes with 5 μm electrode width and spacing. Ti, Ni, and Cr were used as electrode metals. Ti–Ge–Ti case yields the lowest I_{dark}. Inset, current versus voltage characteristics of metal-semiconductor (Ti–Ge) Schottky diode on MHAH-Ge, both forward and reverse bias regions.
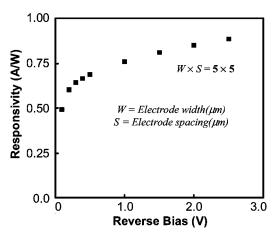
Fig. 3.   Photodetector responsivity at $\lambda = 1.55\,\mu$m versus reverse bias for Ti–Ge–Ti MSM-PDs with $5\,\mu$m finger width and spacing and $10^4\,\mu$m^2 active area.

reflections from the surface. The residual tensile strain in the Ge film, as verified by XRD measurements, further contributes to high $\Re$ at $1.55\,\mu$m, owing to strain-induced bandgap shrinkage.[8]

The optoelectronic quality of the Ge film can also be investigated by measuring the dependence of the photocurrent on the applied electric field (E) and the intensity of light impinging on the sample. The measured I_{photo} versus E is found, for weak fields, to exhibit a linear relation as described by the Hecht formula[9] but saturates for large values of E. Moreover, the photocurrent remains linear for over an order of magnitude in light intensity for various applied voltages. The detectors were not optimized for fast response because of lithographic limitations. Simulations show time response <350 ps at a reverse bias of 2 V, corresponding to a frequency cutoff higher than 1 GHz. Detector bandwidth could be further improved by submicrometer film thickness[4] in trade for responsivity. The performance of our photo-

detectors can be optimized by incorporating different metals to provide work-function asymmetry. This may be helpful in obtaining a built-in E-field, such as in p-i-n detectors, to facilitate low-voltage bias operation.[10]

In summary, we have successfully demonstrated MSM photodetectors in Ge grown directly on Si by using a novel technique that allows growth of high-quality thick heteroepitaxial-Ge layers on Si. Up to 68% quantum efficiency detectors with 0.85 A/W responsivities were achieved at $1.55\,\mu$m. Exceptionally high efficiency of the photodiodes at $1.55\,\mu$m also reveals the high quality of the grown MHAH-Ge layers, making this technology a candidate for monolithic integration of Ge and Si optoelectronics.

A. Okyay's e-mail address is aokyay@stanford.edu.

References

1. S. Luryi, A. Kastalsky, and J. C. Bean, IEEE Trans. Electron Devices **ED-31**, 1135 (1984).
2. S. Fama, L. Colace, G. Masini, G. Assanto, and H. C. Luan, Appl. Phys. Lett. **81**, 586 (2002).
3. L. Colace, G. Masini, G. Assanto, H. C. Luan, K. Wada, and L. C. Kimerling, Appl. Phys. Lett. **76**, 1231 (2000).
4. M. Jutzi, M. Berroth, G. Wöhl, M. Oehme, and E. Kasper, IEEE Photon. Technol. Lett. **17**, 1510 (2005).
5. A. Nayfeh, C. O. Chui, T. Yonehara, and K. C. Saraswat, "A method to grow heteroepitaxial-Ge on Si: Multiple hydrogen annealing for heteroepitaxy (MHAH)," presented at MRS Spring 2005 Conference, San Fransisco, Calif., March 28–April 1, 2005.
6. A. Nayfeh, C. O. Chui, T. Yonehara, and K. C. Saraswat, Appl. Phys. Lett. **85**, 2815 (2004).
7. M. Yamaguchi, A. Yamamoto, M. Tachikawa, Y. Itoh, and M. Sugo, Appl. Phys. Lett. **53**, 2293 (1998).
8. Y. Ishikawa, K. Wada, D. D. Cannon, J. Liu, H. Luan, and L. C. Kimerling, Appl. Phys. Lett. **82**, 2044 (2003).
9. V. Chu, J. P. Conde, D. S. Shen, and S. Wagner, Appl. Phys. Lett. **55**, 262 (1989).
10. C. O. Chui, A. K. Okyay, and K. C. Saraswat, IEEE Photon. Technol. Lett. **15**, 1585 (2003).